

Emilio Andrea Maugeri\*, Jörg Neuhausen, Robert Eichler, Rugard Dressler, Kim Rijpstra, Stefaan Cottenier, David Piguet, Alexander Vögele and Dorothea Schumann

# Adsorption of volatile polonium and bismuth species on metals in various gas atmospheres: Part I – Adsorption of volatile polonium and bismuth on gold

DOI 10.1515/ract-2016-2573

Received January 12, 2016; accepted May 13, 2016

**Abstract:** Polonium isotopes are considered the most hazardous radionuclides produced during the operation of accelerator driven systems (ADS) when lead–bismuth eutectic (LBE) is used as the reactor coolant and as the spallation target material. In this work the use of gold surfaces for capturing polonium from the cover gas of the ADS reactor was studied by thermochromatography. The results show that gaseous monoatomic polonium, formed in dry hydrogen, is adsorbed on gold at 1058 K. Its adsorption enthalpy was calculated as  $-250 \pm 7$  kJ mol<sup>-1</sup>, using a Monte Carlo simulation code. Highly volatile polonium species that were observed in similar experiments in fused silica columns in the presence of moisture in both inert and reducing gas were not detected in the experiments studying adsorption on gold surfaces. PoO<sub>2</sub> is formed in both dry and moist oxygen, and its interaction with gold is characterized by transport reactions. The interaction of bismuth, present in large amounts in the atmosphere of the ADS, with gold was also evaluated. It was found that bismuth has a higher affinity for gold, compared to

polonium, in an inert, reducing, and oxidizing atmosphere. This fact must be considered when using gold as a material for filtering polonium in the cover gas of ADS.

**Keywords:** Polonium, thermochromatography, ADS, MYRRHA.

## 1 Introduction

One of the key issues in energy production by nuclear fission is the treatment of the spent nuclear fuel (SNF). Two main options are currently available: the so-called open fuel cycle, which consists in the direct disposal of SNF in deep geological repositories, and the closed fuel cycle, consisting of reprocessing the SNF to recover fissile and fertile materials for the production of fresh nuclear fuel. Although the volume of waste remaining after the reprocessing, called high level waste (HLW), is reduced to about one fifth of the original SNF, its radiotoxicity is still high and long-lasting (from 100,000 to millions of years [1, 2]) due to the presence of the long-lived minor actinides (MAs) neptunium, americium, and curium and some long-lived fission products (LLFPs), e. g. <sup>129</sup>I and <sup>99</sup>Tc [3].

Several countries pursue the development of new technologies in order to reduce the long-term radiotoxicity of HLW, based on the concept of “partitioning and transmutation”. According to this strategy the long-lived MAs and LLFPs, after being separated from the SNF, are transmuted into stable nuclides or nuclides with much shorter half-lives [3].

Subcritical accelerator driven systems (ADS), together with critical fast reactors, are the main candidates for carrying out the transmutation of MAs and LLFPs.

An ADS [4] consists of a high intensity proton accelerator (beam energy of 0.6–1 GeV and 4–25 mA beam current), a spallation target made of a heavy metal, and a subcritical core where MAs and LLFPs are loaded. The proton beam impinges on the spallation target producing

---

\*Corresponding author: Emilio Andrea Maugeri, Laboratory for Radiochemistry, Paul Scherrer Institut, Villigen PSI, CH-5232 Villigen, Switzerland, E-mail: emilio-andrea.maugeri@psi.ch

Jörg Neuhausen, Rugard Dressler, David Piguet, Alexander Vögele

and Dorothea Schumann: Laboratory for Radiochemistry, Paul Scherrer Institut, Villigen PSI, CH-5232 Villigen, Switzerland

Robert Eichler: Laboratory for Radiochemistry, Paul Scherrer Institut, Villigen PSI, CH-5232 Villigen, Switzerland; and Department for Chemistry and Biochemistry, University of Berne, CH-3012 Bern, Switzerland

Kim Rijpstra: Center for Molecular Modeling (CMM), Ghent University, Technologiepark 903, BE-9052 Zwijnaarde, Belgium

Stefaan Cottenier: Center for Molecular Modeling (CMM), Ghent University, Technologiepark 903, BE-9052 Zwijnaarde, Belgium; and Department of Materials Science and Engineering, Ghent University, Technologiepark 903, BE-9052 Zwijnaarde, Belgium

neutrons, which breed fissile material in the subcritical core and transmute MAs and LLFPs, simultaneously.

In the 1990s the Belgian Nuclear Research Centre SCK·CEN started a project to demonstrate the physical and technological feasibility of an ADS for transmuting long-lived MAs (<http://myrrha.sckcen.be/>). Within this project, a prototype of an ADS called MYRRHA is planned to be built. MYRRHA is an ADS using liquid lead-bismuth eutectic (LBE) as a reactor coolant and as a spallation target material. The main advantages of using LBE are its chemical stability, low melting temperature, high boiling point, low reactivity with water and air and a good neutronic performance [5]. However, the interaction of protons and neutrons with bismuth leads – among others – to the production of  $^{208-210}\text{Po}$ , in both target and coolant. These polonium isotopes are highly radiotoxic, as they are  $\alpha$ -emitters with relatively short half-lives ( $^{210}\text{Po}$ : 138.4 days [6],  $^{209}\text{Po}$ : 125.2 years [6, 7],  $^{208}\text{Po}$ : 2.9 years [6]). Moreover, the polonium has a biological half-life in humans of 30–50 days [8] and has a significant volatility. These physical, chemical and nuclear properties make polonium production a serious safety problem that has to be resolved to proceed with the MYRRHA project. In order to guarantee a safe operation as well as the long-term waste disposal of activated material from an ADS facility, extended R&D work is required to (i) study the release behavior of polonium from the target and the coolant under realistic operational (between 473 and 673 K, inert cover gas, low partial pressure of  $\text{H}_2$  and  $\text{H}_2\text{O}$ ) and accidental conditions (inert or oxidizing gas, possibly high content of  $\text{H}_2\text{O}$ ) and (ii) to find reliable methods to trap released dangerous gas phase species under these conditions.

The evaporation behavior of polonium from liquid lead–bismuth has been studied throughout the last decade. These studies consistently showed that under inert and reducing (typically Ar/5%  $\text{H}_2$ ) conditions and at temperatures higher than 873 K, polonium evaporates from LBE following Henry's law [9–12]. Buongiorno et al., however, indicated that the vapor pressure of polonium could be drastically enhanced by the formation of a more volatile species, possibly  $\text{H}_2\text{Po}$ , in presence of moisture and hydrogen [11]. Also Petryanov et al. reported the formation of a gaseous polonium compound when moist air was blown over polonium containing samples [13]. Maugeri et al. have recently studied the formation of different volatile polonium species, investigating trace amounts of  $^{206}\text{Po}$  using the thermochromatography method [14]. They concluded that in inert gas and hydrogen atmospheres and in the absence of moisture, polonium is present in the gas-phase in its monoatomic form. No indications of the formation of  $\text{H}_2\text{Po}$  were found in these experiments.

However, when traces of moisture are present in the gas phase, molecular polonium containing species are formed which are more volatile than monoatomic polonium. As the formation of these volatile compounds is enhanced by the presence of moisture, the authors tentatively assigned them to be polonium hydroxides.

Pankratov et al. gave an overview on the problems related to the volatility of polonium in nuclear power systems during normal operating, maintenance, reloading of nuclear fuel, interloop leakage or accidental spilling of radioactive coolant [15]. To reduce the risk of polonium contamination during maintenance or in case of accidents [16], its removal from LBE by various methods was considered [17, 18]. As none of those methods may guarantee a complete removal of polonium from LBE, filtering of the gas phase must be taken into account. Obara et al. proposed stainless steel wire mesh for the removal of polonium from the gas phase [19]. The authors claim that between 88 and 97% of polonium in the gas phase could be removed by this filtering system at “filter temperatures” between 503 and 878 K. Unfortunately, no thermodynamic parameters have been evaluated from this observation. Furthermore, the relative amount of polonium trapped by the stainless steel wire mesh is not referred to the total quantity of polonium in the gas phase (released from a neutron irradiated LBE sample at 823 K). Thus, there is no guarantee that all chemical states of polonium present in the gas phase between 503 and 878 K are caught by the filter.

In this work, we study metallic gold surfaces as a potential material for trapping polonium, as when compared to steel and copper it is known to provide a very stable metallic surface even in oxidizing gas phase conditions. The interaction between polonium and gold under inert conditions was already investigated in previous works. Gägger et al. [20] measured a value of  $-224 \pm 11 \text{ kJ mol}^{-1}$  for the adsorption enthalpy of polonium on gold, using the on-line isothermal gas-adsorption chromatography method with helium as a carrier gas. In the same work, they derived two values for the adsorption enthalpy of polonium on gold ( $-196$  and  $-226 \text{ kJ mol}^{-1}$ ) from the desorption temperatures of polonium from gold previously reported [21, 22], using a model presented [23]. Eichler et al. [23] calculated the adsorption enthalpy of polonium on gold as  $-200 \text{ kJ mol}^{-1}$ , using a semi-empirical model considering the desublimation enthalpy, enthalpy of solution at infinite dilution of polonium in solid gold and segregation energy required for the formation of the adsorbed state from the solid solution.

Compared to the earlier studies that used inert carrier gases, in the present work, we study, for the first time, the formation of a volatile polonium species at varied redox potential and their interaction with the gold surface.

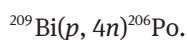
Thermochromatography was used to investigate their adsorption interaction with gold. The aim is to simulate the behavior of gold as a filtering material under various operation and accident scenarios for an ADS mentioned above.

Moreover, the design of a gas phase filtering system of an ADS will have to be operated in an environment with high concentrations of bismuth (several orders of magnitude higher than polonium). Therefore, in this work, the adsorption interaction of trace amounts of bismuth with gold was also studied by thermochromatography, considering all the different conditions evaluated for polonium.

## 2 Experimental

### 2.1 Sample preparation

The isotope  $^{206}\text{Po}$  was used for thermochromatographic investigations because of its easily detectable  $\gamma$ -ray emission and the suitable half-life of 8.8 days. The isotope was obtained by irradiation of bismuth metal disks with a 40 MeV proton beam of up to  $3\ \mu\text{A}$  current at ZAG Karlsruhe according to the nuclear reaction:



The irradiated bismuth disks (Goodfellow, 99.9999% purity) had an average diameter of  $\sim 10$  mm and a thickness of  $\sim 0.5$  mm. About 1 MBq ( $1.097 \times 10^{12}$  atoms) of  $^{206}\text{Po}$  were produced in each disk. Thus, the obtained samples consist of large (macroscopic amounts) bismuth matrices containing trace amounts of  $^{206}\text{Po}$ . Each irradiated disk was cut in small fragments containing between 5 and 20 kBq of  $^{206}\text{Po}$  suitable for one thermochromatography experiment.

It is necessary to avoid that macroscopic amounts of bismuth are transported to and deposited in the stationary phase (gold column) during the thermochromatography experiments. These would alter the stationary phase and prevent the interaction between polonium and gold, thus altering the thermochromatography results. Therefore, it was necessary to separate polonium from the bismuth matrix before starting the thermochromatography experiments.

An efficient separation of bismuth and polonium by thermal release has been proven [9].

In the present work, polonium was separated from bismuth using the setup depicted in Figure 1, consisting of a fused silica tube (1) placed in a tubular furnace (2). The irradiated bismuth (4) was heated to 1123 K under a constant flow of untreated helium (Messer® 5.0) at ambient pressure for 1 h. The temperature of the irradiated bismuth was continuously measured by a type K thermocouple (3).

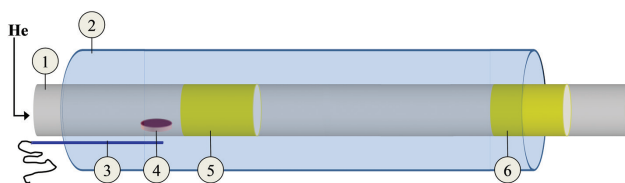


**Figure 1:** Polonium separation set-up: fused silica tube (1); tubular furnace (2); thermocouple (3); irradiated bismuth,  $T = 1123$  K, (4); gold foil used to trap the bismuth evaporated during the separation,  $T = 1123$  K (5); gold foil used to collect the polonium separated from the bismuth matrix,  $800\ \text{K} > T > 550\ \text{K}$  (6).

Polonium evaporated from the irradiated bismuth was deposited on a gold foil placed at the end of the fused silica tube (6), at a temperature of approximately 800 K. An additional gold foil was placed in the fused silica tube at  $1123 \pm 10$  K (5) to trap the bismuth evaporated during the heating of the irradiated sample. The polonium deposited on the second gold foil (6) was used for thermochromatography experiments as starting material.

For the purpose of studying bismuth-adsorption on gold, in some cases the samples of polonium deposited on gold were stored for about 2 days prior to the thermochromatography experiment to obtain  $^{206}\text{Bi}$  from the decay of  $^{206}\text{Po}$  according to  $^{206}\text{Po}(\epsilon; \beta^+)^{206}\text{Bi}$ .  $^{206}\text{Bi}$  decays to  $^{206}\text{Pb}$  with a half-life of 6.2 days according to  $^{206}\text{Bi}(\epsilon; \beta^+)^{206}\text{Pb}$ , emitting  $\gamma$ -rays suitable for its detection in thermochromatographic investigations.

### 2.2 Thermochromatography

In thermochromatography (TC) experiments, a trace amount of the investigated species (“a concentration of element or compound so low that it makes the collisions between two identical tracer entities in the course of a real experiment completely improbable” [24]) is desorbed from a starting phase and transported by a carrier gas into a column (stationary phase) placed in a negative temperature gradient. This species undergoes an adsorption–desorption equilibrium with the stationary phase, which is a function of its molecular weight, free surface of the stationary phase, temperature and gas flow. After a certain experiment time, the species will adsorb on a specific region of the stationary phase, characterized by a defined temperature. Thus, the result of a TC experiment consists of a thermochromatogram in which the deposition pattern of the adsorbed species is plotted as a function of either its position in the column or its deposition temperature. If the chemical state of the investigated species is preserved throughout the experiment, the obtained thermochromatogram is typically characterized by a single sharp peak. The shape of the deposition peak

depends on the gas flow and temperature gradient of the stationary phase. At the gas flow conditions used in this work, a single species is estimated to be deposited within 3–5 cm (depending on the local temperature gradient, which is not necessarily constant along the stationary phase).

The adsorption/desorption equilibrium can be superimposed by chemical reactions with components of a reactive gas mixture, leading to a transport reaction. In this case, a broadening of the deposition patterns in the thermochromatogram is observed that is influenced by the reaction kinetics and thus is a function of the partial pressure of the reactive component in the carrier gas [25].

In the case of a simple adsorption/desorption equilibrium without superimposed chemical reactions it is possible to determine from the obtained thermochromatogram the adsorption enthalpy of the deposited species using a Monte Carlo simulation method for gas chromatography developed by Zvara [26], which simulates the adsorption–desorption interaction of each individual species with the stationary phase during the experiment. Results with superimposed transport reaction have to be evaluated by the thermodynamic model presented for instance [25, 27].

The main source of uncertainty is the measurement of the deposition temperature of  $\pm 30$  K under the conditions used in this work. This experimental uncertainty causes an uncertainty on the calculated adsorption enthalpy of about 7–10 kJ mol<sup>-1</sup>.

The thermochromatography setup used in this work is schematically illustrated in Figure 2. It consists of a fused silica tube (1) (i. e.  $d = 5$  mm,  $l = 104$  cm), encapsulated in an Inconel® tube placed in a negative temperature gradient furnace (2), with a temperature profile ranging from a maximum temperature of 1227 to minimum temperature of 168 K. The column was lined inside with gold foil (Goodfellow, thickness  $0.020 \pm 0.003$  mm, purity 99.9%) along the entire temperature gradient, from 1227 to 168 K (3).

Before each experiment, the gold column was heated up to 1273 K under a constant flow of hydrogen, to remove impurities from its surface. Then the tube was flushed with pure helium at the same temperature to remove the hydrogen adsorbed on the surface or dissolved in the bulk of the gold in order to avoid reactions of polonium with hydrogen during the thermochromatography experiments performed in non-H<sub>2</sub>-containing carrier gases. The tube was finally cooled down to room temperature under a helium flow.

The samples were placed in the starting position of the thermochromatography setup, 0 cm (4), and heated up to 1227 K while, at the same time, a stable thermal gradient was established in the gold tube. Each experiment was performed for 2.5 h. The setup was equipped with a

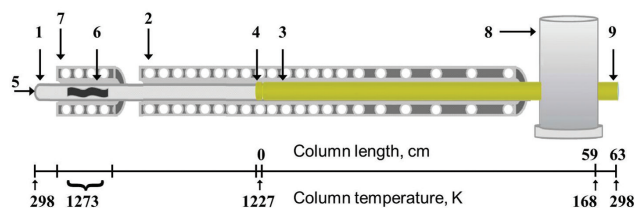


**Figure 2:** Thermochromatography set-up: fused silica tube (1); negative gradient furnace (2); gold tube (1227–168 K) (3); starting phase (1227 K) (4); carrier gas inlet (He, H<sub>2</sub>, O<sub>2</sub>) (5); tantalum getter (6); getter furnace (1273 K) (7); liquid nitrogen cryostat (168 K) (8); carrier gas outlet (9).

carrier gas supply (5) connected by Swagelok® components to the Inconel® steel tube, allowing for the use of different atmospheres, namely inert, reducing, oxidizing, moist, and dry. The set up was flushed with the carrier gas for 15 min before each experiment. The flow rate of the carrier gas was controlled using a mass flow controller set to a flow rate of 25 mL min<sup>-1</sup> for all the experiments. The inert (He, Messer® 5.0) and reducing (H<sub>2</sub>, Messer® 5.0) carrier gases were passed through a purification system consisting of a P<sub>2</sub>O<sub>5</sub> (SICAPENT®) cartridge (not shown) and a Ta getter (6) heated to 1273 K by an additional furnace (7) to remove residual moisture and oxygen. Oxygen (Messer® 5.0) used as a carrier gas was only dried by passing through the SICAPENT® cartridge. When using moisturized gases, the carrier gas was passed through a reservoir with a stationary vapor pressure over liquid water held at defined temperatures (not shown in Figure 2) bypassing the purification system.

The distribution of the adsorbed species in the fused silica tube was detected by successively screening small sections of the column using standard  $\gamma$ -spectrometry with a lead collimator (window size 1 cm  $\times$  1 cm, lead thickness 1 cm) placed in front of an HPGe-detector with a resolution of 2.13 keV at 1.33 MeV controlled by Canberra's Genie2K® software package.

To measure <sup>206</sup>Po the X-ray line Bi K<sub>α1</sub> at 77.1 keV was used, while the  $\gamma$ -line at 184 keV was used to detect <sup>206</sup>Bi.

## 3 Results

### 3.1 Separation of polonium from bismuth matrix

After performing the separation procedure described above, no polonium was detected neither on the gold foil placed in the high temperature section of the silica tube (5), Figure 1, nor on the silica tube itself. Typically  $94 \pm 2\%$  of the polonium present in the irradiated bismuth was

recovered on the gold foil designated “starting material” (6) located at the low temperature section of the silica tube.

The amount of bismuth transported to the starting material of the thermochromatography experiment during the separation procedure was deduced by measuring the  $^{207}\text{Bi}$  activity during all the steps of the separation process. The activity of  $^{207}\text{Bi}$  measured on the starting material after separations was typically lower than 0.2 Bq. Thus, the amounts of macroscopic Bi present in the experiments could be evaluated.

### 3.2 Thermochromatography study of polonium and bismuth on gold

The interaction between polonium and bismuth with gold was investigated under inert, reducing and oxidizing conditions, with different levels of moisture. At least two experiments for each considered condition were performed in order to verify the reproducibility of the obtained results.

In this section, first the thermochromatograms of  $^{206}\text{Po}$  obtained in purified hydrogen, helium and oxygen are presented followed by the results obtained in moist gases. Afterwards, the thermochromatograms of  $^{206}\text{Bi}$  in purified hydrogen, helium and oxygen, are presented.

Table 1 summarizes the experimental conditions and the results of the  $^{206}\text{Po}$  investigations, in terms of deposition temperature, adsorption enthalpy and chemical speciation.

Figure 3 shows the results of Exp. I–VI, where thermochromatograms of  $^{206}\text{Po}$  were obtained using purified  $\text{H}_2$  (a) and He (b) and dry  $\text{O}_2$  (c) as a carrier gas.

The thermochromatograms of Exp. I and II (A) show a single sharp peak, centered at 1058 K. Using the Monte

Carlo code [26], adsorption enthalpies of the deposited species were calculated as  $-246 \pm 7$  and  $-254 \pm 7$   $\text{kJ mol}^{-1}$ , respectively.

The thermochromatograms of  $^{206}\text{Po}$  obtained using purified helium as a carrier gas, Exp. III and Exp. IV, are presented in Figure 3b. They show a sharp peak centered at 865 and 897 K, respectively. Using the Monte Carlo code [26], adsorption enthalpies of  $-207 \pm 7$  and  $-214 \pm 7$   $\text{kJ mol}^{-1}$  were calculated for the Exp. III and IV, respectively.

Exp. V and VI were performed using dry oxygen as a carrier gas. The obtained thermochromatograms, Figure 3c, reveal a deposition peaking between 967 and 937 K. The adsorption enthalpies of the deposited species were calculated as  $-224 \pm 7$   $\text{kJ mol}^{-1}$  and  $-231 \pm 7$   $\text{kJ mol}^{-1}$ , respectively.

Exp. VII and VIII were performed using moist  $\text{H}_2$  as a carrier gas. Figure 4a shows the obtained thermochromatograms, characterized by the presence of a sharp deposition pattern centered at  $1058 \pm 30$  K and  $1030 \pm 30$  K, respectively. Their corresponding adsorption enthalpies were calculated as  $-249 \pm 7$  and  $-243 \pm 7$   $\text{kJ mol}^{-1}$ .

Exp. IX and X were performed using moist helium as a carrier gas. The two obtained deposition patterns, Figure 4b, show a main deposition centered at 1026 K. The adsorption enthalpies were calculated as  $-238 \pm 7$  for both experiments.

In Exp. XI and XII moist  $\text{O}_2$  was used as a carrier gas. Figure 4c shows the obtained thermochromatograms, characterized by a broad deposition pattern peaking at 967 K. Two values of adsorption enthalpies were calculated, i. e.  $-230 \pm 7$  and  $-226 \pm 7$   $\text{kJ mol}^{-1}$ , for Exp. XI and XII, respectively.

The starting materials of Exp. I, III and V were stored for about 2 days prior to the thermochromatography

**Table 1:** Experimental conditions and the results of the  $^{206}\text{Po}$  investigations.

Sample number	Carrier gas	$^aT_{\text{dep}}^{206}\text{Po}/\text{K}$ (uncertainty = $\pm 30$ K)	$\Delta H_{\text{ads}}/\text{kJ mol}^{-1}$ (uncertainty = $\pm 7$ $\text{kJ mol}^{-1}$ )	Chemical species
Exp. I	Purified $\text{H}_2$	1058	-246	Po
Exp. II		1058	-254	
Exp. III	Purified He	865	-207	BiPo
Exp. IV		897	-214	
Exp. V	Dry $\text{O}_2$	937	-224	$\text{PoO}_2$
Exp. VI		967	-231	
Exp. VII	Moist $\text{H}_2$	1058	-249	Po
Exp. VIII		1030	-243	
Exp. IX	Moist He	1026	-238	Po or $\text{PoO}_2$
Exp. X		1026	-238	
Exp. XI	Moist $\text{O}_2$	967	-230	$\text{PoO}_2$
Exp. XII		967	-226	

<sup>a</sup>The deposition temperature,  $T_{\text{dep}}$  is considered as the temperature corresponding to maximum in the polonium deposition pattern. Considering the uncertainties of temperature and position measurement, its uncertainty is estimated to be  $\pm 30$  K.

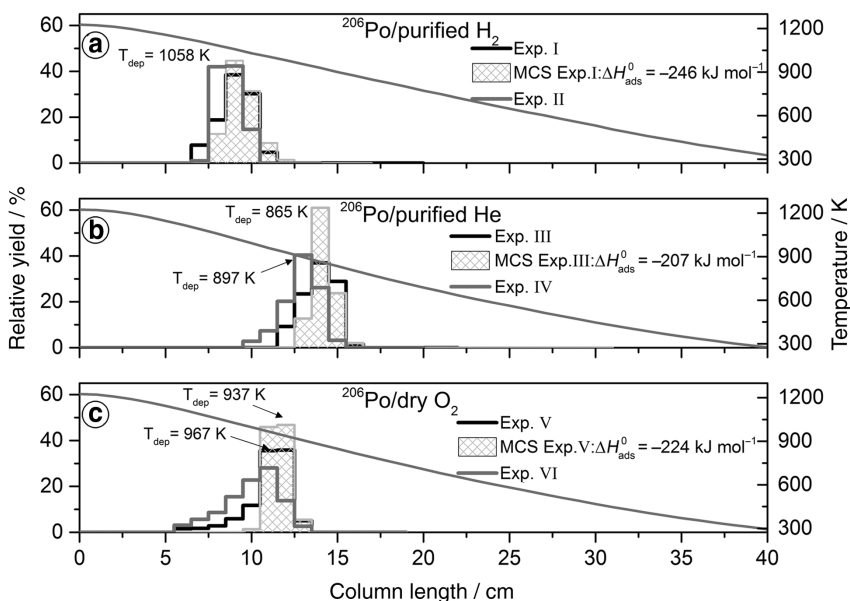


**Figure 3:** Thermochromatograms of  $^{206}\text{Po}$  on gold. (a) Purified  $\text{H}_2$  as a carrier gas: Exp. I (black bars) and Exp. II (gray bars). Light gray cross-hatched bars represent the Monte Carlo simulation of Exp. I. (b) Purified He as a carrier gas: Exp. III (black bars) and Exp. IV (gray bars). Light gray cross-hatched bars represent the Monte Carlo simulation of Exp. III. (c) Dry  $\text{O}_2$  as a carrier gas: Exp. V (black bars) and Exp. VI (gray bars). Light gray cross-hatched bars represent the Monte Carlo simulation of Exp. V.

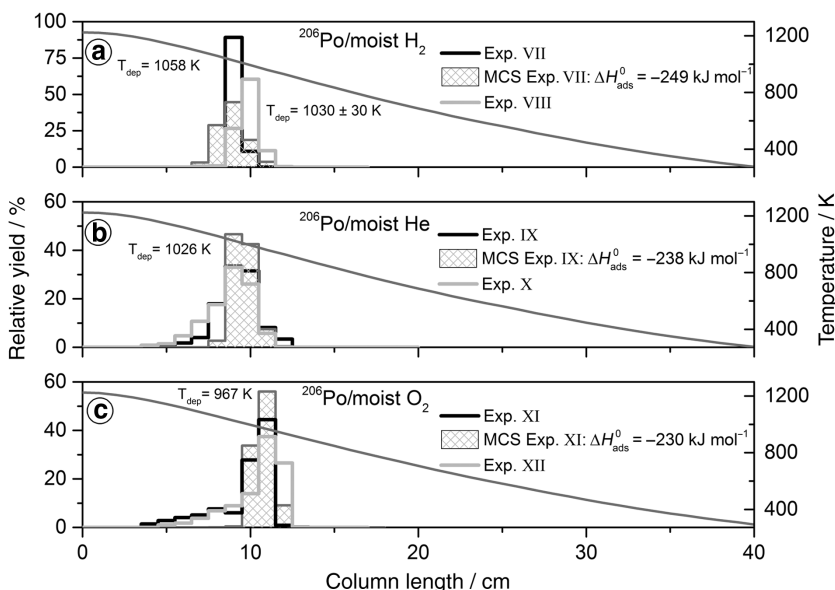


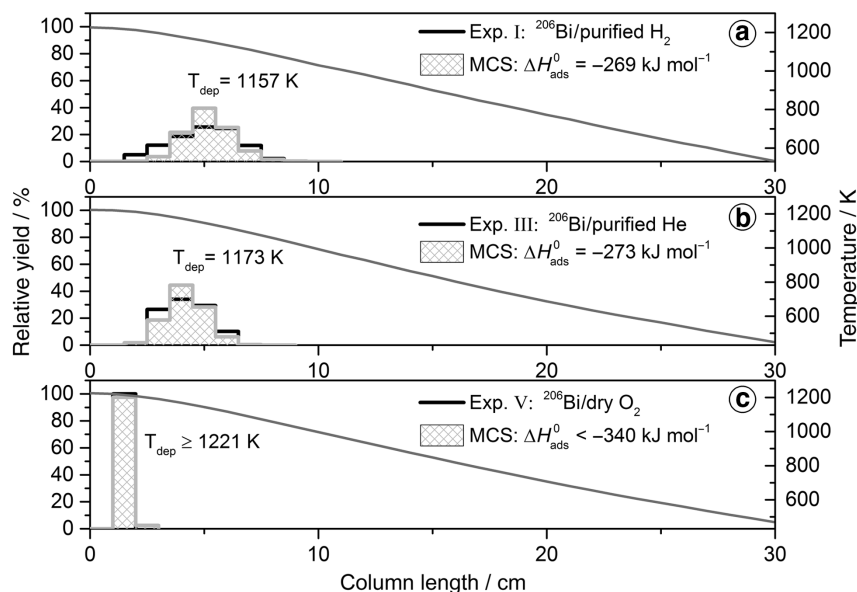
**Figure 4:** Thermochromatograms of  $^{206}\text{Po}$  on gold. (a) Moist  $\text{H}_2$  as a carrier gas: Exp. VII (black bars) and Exp. VIII (gray bars). Light gray cross-hatched bars represent the Monte Carlo simulation of Exp. VII. (b) Moist He as a carrier gas: Exp. IX (black bars) and Exp. X (gray bars). Light gray cross-hatched bars represent the Monte Carlo simulation of Exp. IX. (c) Moist  $\text{O}_2$  as a carrier gas: Exp. XI (black bars) and Exp. XII (gray bars). Light gray cross-hatched bars represent the Monte Carlo simulation of Exp. XI.

experiments to obtain  $^{206}\text{Bi}$  and to study its interaction with gold using the same purified  $\text{H}_2$ , He and dry  $\text{O}_2$ , respectively. Table 2 summarizes the experimental conditions and the results obtained in terms of deposition temperature, adsorption enthalpy and presumed chemical speciation.

The obtained thermochromatograms of Exp. I and III (a and b in Figure 5) show deposition patterns centered at 1157 and 1173 K, respectively, while the deposition pattern obtained for Exp. V (c in Figure 5), shows that practically all the bismuth was deposited in the first centimeter of the gold column at 1221 K.

**Table 2:** Experimental conditions and the results of the  $^{206}\text{Bi}$  investigations.

Sample number	Carrier gas	$T_{\text{dep}} \text{ } ^{206}\text{Bi}/\text{K}$	$\Delta H_{\text{ads}}^0 / \text{kJ mol}^{-1}$	Chemical species
Exp. I	Purified $\text{H}_2$	1157	$-269 \pm 7$	Bi
Exp. III	Purified He	1173	$-273 \pm 7$	Bi
Exp. V	Dry $\text{O}_2$	$\geq 1221$	$\leq -340 \pm 7$	Bi-oxide

**Figure 5:** Thermochromatograms of  $^{206}\text{Bi}$  on gold using purified:  $\text{H}_2$  (a), He (b) and dry  $\text{O}_2$  (c) as a carrier gas, respectively. The light gray cross-hatched bars represent relative Monte Carlo simulations.

## 4 Discussion

### 4.1 Separation of polonium from bismuth matrix

The obtained results show that the used separation technique allows to recover about  $94 \pm 2\%$  of the polonium present in the irradiated bismuth on the gold foil used as the “starting material”.

It is not possible to determine in which chemical form polonium is present in the starting material. In fact polonium could be evaporated from the irradiated bismuth and deposited on the starting material as either monoatomic polonium or as bismuth polonide.

The amount of bismuth transported onto the starting material during the separation process is an important factor for the evaluation of the thermochromatographic results because the bismuth may form a layer on the gold surface used as stationary phase during the thermochromatographic experiment, changing the sorption behavior of polonium.

Based on the metallic radius of bismuth and the lattice constant of solid gold, it was calculated that

approximately  $2 \times 10^{15}$  bismuth atoms would be required to form a monolayer on a section of 1 cm length of the gold column.

The activity of  $^{207}\text{Bi}$  measured on the starting material after separation was typically lower than 0.2 Bq, corresponding to a maximum number of bismuth atoms of about  $4 \times 10^{15}$ .

As an example, we present the results of a separation Bi–Po from an irradiated bismuth sample (0.1131 g,  $3.3 \times 10^{20}$  atoms of  $^{\text{nat}}\text{Bi}$ ). The activity of  $^{207}\text{Bi}$  was measured by  $\gamma$ -spectroscopy before the separation as 16 kBq ( $2.3 \times 10^{13}$  atoms  $^{207}\text{Bi}$ ). Thus, the ratio of  $^{\text{nat}}\text{Bi}/^{207}\text{Bi}$  atoms was  $1.4 \times 10^7$ .

Then, the sample was heated at 1223 K under a constant flow of helium for 1 h, in the set-up illustrated in Figure 1 (Section 2.1). At the end of the separation, the activity of  $^{207}\text{Bi}$  on the gold foil (6 in Figure 1) was measured by  $\gamma$ -spectroscopy as 0.20 Bq. Considering the ratio  $^{\text{nat}}\text{Bi}/^{207}\text{Bi}$  did not change, the number of  $^{\text{nat}}\text{Bi}$  atoms in the starting material was calculated as  $3.9 \times 10^{15}$ .

This amount of bismuth is enough to form a monolayer of maximum 2 cm length in the gold column, thus it will not interfere with the polonium–gold adsorption–desorption

interaction during the thermochromatography experiments if considering the lateral separation in the thermochromatography column.

The mole fraction of polonium in the starting material is in the range of  $1.4\text{--}5.6 \times 10^{-6}$ . Thus, the starting material is a dilute solution of polonium in bismuth. This supports the idea that polonium could evaporate as bismuth polonide rather than monoatomic polonium if the bismuth–polonide molecules are reasonably stable.

## 4.2 Thermochromatography study of polonium and bismuth on gold

The obtained results of Exp. I–II and Exp. III–IV clearly indicate two different polonium containing species formed when using reducing ( $\text{H}_2$ ) and inert (He) carrier gases, respectively. The two species are characterized by two different values of adsorption enthalpies,  $-250 \pm 10 \text{ kJ mol}^{-1}$  (average of the values calculated for Exp. I and II) and  $-210 \pm 10 \text{ kJ mol}^{-1}$  (average of the values calculated for Exp. III and IV), respectively.

Considering that substantial amounts of bismuth are present in the starting material and the amount of polonium present is so small that species containing more than one polonium atom can be excluded, the most probable species that can occur in the thermochromatographic experiments are monoatomic polonium and diatomic BiPo molecules. In a similar way, Maugeri et al. [14], studying the interaction of polonium with fused silica using a similar set-up, concluded that under reducing and inert conditions in the absence of moisture, either polonium or bismuth polonide is formed and deposited on fused silica. Thus, the species formed and deposited on gold in Exp. I to IV could be either monoatomic polonium or BiPo.

However, it is more likely that a molecular species such as BiPo remains intact and is deposited on gold as a molecule in an inert gas, i. e. in Exp. III and IV, while in a reactive gas such as hydrogen it seems more likely that the molecule can disintegrate, forming transient hydride species that might decompose almost immediately ( $\text{PoH}_2$  is known to be thermally unstable [28]), finally leading to the deposition of polonium on gold. The results of a quantum mechanical study of the adsorption of monoatomic polonium and simple polonium containing molecules on gold surfaces based on density functional theory (DFT) indicates that the BiPo molecule should not fully dissociate when adsorbed on the gold surface, qualitatively supporting the assumption that an adsorption/desorption equilibrium involving BiPo can exist [29]. On the other hand, the calculated adsorption enthalpy of

$-287 \text{ kJ mol}^{-1}$  is not in agreement with our observation. Furthermore, the adsorption enthalpy of  $-245 \text{ kJ mol}^{-1}$  predicted in the same DFT study for monoatomic polonium on gold (110-surface of a gold slab) is in very good agreement with the value of adsorption enthalpy deduced from Exp. I and II. Thus, it seems most likely that the polonium species deposited when using  $\text{H}_2$  as a carrier gas, Exp. I and II, is monoatomic polonium, whereas under inert gas atmosphere the diatomic BiPo molecule evaporated from the starting material could be preserved.

According to Eichler [30] two types of adsorption processes must be considered: adsorption in and on the surface. These two processes can be discriminated according to the relative value of the partial molar solution enthalpy of the solute (polonium) in the solid phase (gold),  $\Delta H_{LS}$ .

If  $\Delta H_{LS}$  is lower than  $50 \text{ kJ mol}^{-1}$ , the formation of a stable intermetallic compound in the solid phase is favoured, suggesting an adsorption in the surface. If the  $\Delta H_{LS}$  is higher than  $50 \text{ kJ mol}^{-1}$ , stable intermetallic compounds are not expected to form and an adsorption on the surface is more favorable. Neuhausen and Eichler [31], using the model described [32], calculated the  $\Delta H_{LS}$  for polonium in gold as  $47 \text{ kJ mol}^{-1}$ . Using this value in the semi-empirical model described [33] it is possible to calculate the adsorption enthalpy of polonium on gold. It is important to notice that the value of  $\Delta H_{LS}$  calculated by Neuhausen and Eichler [31] for polonium on gold,  $47 \text{ kJ mol}^{-1}$ , is just at the limit between the two possible adsorption scenarios in and on the surface (see supplementary material). Thus, both values of the corresponding adsorption enthalpies were derived as  $-183$  and  $-274 \text{ kJ mol}^{-1}$ , respectively. The last value,  $-274 \text{ kJ mol}^{-1}$ , is in fair agreement with the adsorption enthalpy determined in this work ( $-250 \text{ kJ mol}^{-1}$ ), indicating that polonium is more likely being adsorbed on the gold surface.

Exp. V and VI were performed using dry oxygen as a carrier gas. The obtained thermochromatograms, Figure 3c, reveal deposition patterns peaking at 967 and 937 K, respectively. The adsorption enthalpies of the deposited species were calculated as  $-224 \pm 7$  and  $-231 \pm 7 \text{ kJ mol}^{-1}$ , for Exp. V and VI, respectively, assuming an unchanged stable chemical state of the species. Considering the uncertainties of the calculated adsorption enthalpies, the deposited species is considered to be the same in both experiments.

The most stable valence state of polonium in pure oxygen carrier gas is +4 [34]. Therefore, the deposited polonium species is considered to be  $\text{PoO}_2$ . Both deposition patterns show a tailing at high temperature indicating that the main deposited species,  $\text{PoO}_2$ , could be the

result of a transport process. The adsorption enthalpy values indicate that  $\text{PoO}_2$ , if formed in the cover gas of the ADS reactor, has a lower affinity for gold compared to polonium but higher than BiPo.

Exp. VII and VIII were performed using moist  $\text{H}_2$  as a carrier gas. Figure 4d show the obtained thermochromatograms characterized by the presence of a sharp deposition pattern centered at  $1058 \pm 30$  K and  $1030 \pm 30$  K, respectively. The sharpness of the obtained thermochromatograms indicates that only one single polonium species was deposited on gold in each experiment. Values of adsorption enthalpy of  $-249 \pm 7$  and  $-243 \pm 7$   $\text{kJ mol}^{-1}$  were calculated for the Exp. VII and VIII, respectively. Considering the uncertainties of the calculated adsorption enthalpies,  $\pm 7$   $\text{kJ mol}^{-1}$ , these species are considered to be the same. The average value of adsorption enthalpy,  $-246 \pm 10$   $\text{kJ mol}^{-1}$ , is very close to the one determined in Exp. I and II for monoatomic polonium,  $-250 \pm 7$   $\text{kJ mol}^{-1}$ . Thus, the species deposited on gold when using moist  $\text{H}_2$  as a carrier gas is considered to be monoatomic polonium.

Exp. IX and X, performed using moist He as a carrier gas, resulted in thermochromatograms centered at  $1026 \pm 30$  K with a small tailing towards high temperature. An adsorption enthalpy of  $-238 \pm 7$   $\text{kJ mol}^{-1}$  was calculated for both experiments.

In this case the obtained adsorption enthalpy of the deposited species is in between those obtained for monoatomic polonium and for  $\text{PoO}_2$ . Thus, it is not possible to assign the species. It is noteworthy that the addition of a reactive component such as moisture to the inert gas leads to a different result compared to the pure inert gas Exp. III and IV. Qualitatively, the results found in moist helium are compatible with the view outlined above that diatomic BiPo molecules are decomposed by reactive gases. The tailing could be the result of the formation of transient species that are longer lived than those formed during the decomposition of BiPo in moist  $\text{H}_2$ .

Maugeri et al. reported the formation of different polonium species with significantly higher volatility compared to monoatomic polonium when both moist helium and moist  $\text{H}_2$  are used as a carrier gas in thermochromatography experiments in fused silica columns [12]. This effect is not observed when using gold as the stationary phase, indicating that these more volatile polonium species, if formed, decompose on the gold surface to monoatomic polonium.

Figure 4c shows the thermochromatograms obtained when moist  $\text{O}_2$  is used as a carrier gas, Exp. XI and XII. In this case the deposition patterns are characterized as a sharp peak centered at  $967 \pm 30$  K with a tail at higher temperature, between 1027 and 1169 K. The Monte Carlo simulation of the sharp peak gives a value of adsorption

enthalpy of  $-228 \pm 10$   $\text{kJ mol}^{-1}$  (average of the values calculated for Exp. XI and XII, see Table 1), assuming an unchanged stable chemical state of the species. This result indicates that the deposited species is  $\text{PoO}_2$  ( $\Delta H_{\text{ads}} = -227.5 \pm 10$   $\text{kJ mol}^{-1}$ , average of the values calculated for Exp. V and VI). The tail at high temperature indicates that, like when using purified  $\text{O}_2$  (see Exp. V and VI) the main deposited species,  $\text{PoO}_2$ , could be the result of a transport process.

The adsorption of bismuth on gold was studied in reducing, inert and oxidizing conditions in Exp. I, III, and V, respectively. The thermochromatograms of  $^{206}\text{Bi}$  obtained for Exp. I and III, Figure 5a and b, show a peak centered at 1157 and 1173 K, respectively. The Monte Carlo simulation of Exp. I gives an adsorption enthalpy of  $-269 \pm 7$   $\text{kJ mol}^{-1}$ . Considering the reduction potential of the used carrier gas, the adsorbed species was attributed to bismuth. The Monte Carlo simulation of Exp. III derives an adsorption enthalpy of  $-273 \pm 7$   $\text{kJ mol}^{-1}$ . Considering the uncertainty of the calculated adsorption enthalpy of  $\pm 10$   $\text{kJ mol}^{-1}$ , the adsorbed species is considered to be the same of the Exp. I, i. e. bismuth.

Using the value of  $\Delta H_{\text{LS}}$  of bismuth on the gold surface reported [30] as  $-12$   $\text{kJ mol}^{-1}$  (which indicates that bismuth is adsorbed in the gold surface) in the semi-empirical model described [33], an adsorption enthalpy of bismuth on gold of  $-257$   $\text{kJ mol}^{-1}$  was calculated, which is in very good agreement with the value obtained in this work.

These results agree also very well with the value for the adsorption enthalpy of bismuth on gold calculated in the DFT study [29] as  $-280$   $\text{kJ mol}^{-1}$ , indicating that bismuth has higher affinity for gold than polonium.

The gas phase filtering system of an ADS will potentially work in an environment with a gas phase concentration of bismuth several orders of magnitude higher than polonium. Considering an operational temperature range between 473 and 673 K, an equilibrium vapor pressure of Bi between  $2 \times 10^{-11}$  Pa and  $2 \times 10^{-5}$  Pa can be calculated using Henry constant data from [35], while for Po, assuming a molar fraction of  $10^{-7}$  [36], an equilibrium vapor pressure between  $7 \times 10^{-15}$  Pa and  $1 \times 10^{-9}$  Pa can be calculated using the Henry constant data [35]. This estimation however, relies on extrapolating the temperature functions of the Henry constants to low temperature and furthermore it neglects the formation of more volatile polonium species that have been observed in the relevant temperature range in recent experimental studies [14, 36, 37]. Unfortunately, with the currently existing knowledge, the gas phase concentration of these volatile polonium species cannot be reliably estimated.

Thus, if indeed a filter system using gold surfaces is considered, one has to take into account that it could be contaminated with large amounts of bismuth, altering the adsorption behavior of polonium.

Rijpstra has calculated using DFT methods that if 50% of the gold surface atoms (100-surface of a gold slab) were hypothetically substituted with bismuth atoms, the adsorption enthalpy of polonium would decrease from  $-243 \text{ kJ mol}^{-1}$  (100% gold atoms) to  $-183 \text{ kJ mol}^{-1}$ , while if the complete surface was covered by bismuth atoms the adsorption enthalpy of polonium would drop to  $-177 \text{ kJ mol}^{-1}$  [29]. However, the still strongly negative adsorption enthalpies predicted for bismuth-polluted surfaces indicate that even if the adsorption enthalpy of polonium decreases on gold surfaces polluted with bismuth, polonium could be still removed efficiently from the gas phase.

The thermochromatogram of  $^{206}\text{Bi}$  in Exp. V, Figure 5c, reveals the formation of a single species deposited in the first centimeter of the gold tube, at a temperature of 1223 K. It was not possible to perform an experiment using higher maximum temperature of the gradient due to the melting point of gold, 1337 K. Thus, the derived adsorption enthalpy,  $-340 \text{ kJ mol}^{-1}$ , must be considered as a upper limit. This value was associated to the adsorption of a Bioxide on gold and indicates that this species is the least volatile one among all those observed within the present study.

## 5 Summary and conclusions

In pure hydrogen atmosphere, monoatomic polonium and bismuth are deposited on gold at  $1058 \pm 30 \text{ K}$  and  $1157 \pm 30 \text{ K}$ , respectively. Using a Monte Carlo code their adsorption enthalpies on gold were calculated as  $-250 \pm 7 \text{ kJ mol}^{-1}$  and  $-269 \pm 7 \text{ kJ mol}^{-1}$ , respectively. This indicates that bismuth has a stronger affinity to gold than polonium. This observation must be considered when using gold as a material for filtering polonium in the cover gas of ADS when LBE is used as spallation target and coolant. In fact, bismuth evaporated from the LBE could saturate the gold surface of the filtering system, preventing or altering the adsorption of polonium.

In moist hydrogen and helium atmosphere deposition patterns similar to those observed in pure hydrogen were found, indicating that at these conditions also monoatomic polonium is deposited.

On the contrary, in pure helium a deposition at significantly lower temperature ( $865\text{--}897 \text{ K}$ ) was observed. This finding was tentatively attributed to the chromatographic

transport and deposition of BiPo, being stable at these chemical conditions.

The highly volatile species that were previously observed in thermochromatography experiments using fused silica stationary surfaces were not observed in this work. Either they are decomposed on the gold surface into monoatomic polonium or  $\text{PoO}_2$ , or they are not formed at the high temperatures where adsorption of polonium and  $\text{PoO}_2$  occurs on gold. This indicates that a hot gold surface can be used for trapping polonium species at the studied gas phase compositions. Preliminary tests, placing gold pieces of 1 cm length in a fused silica thermochromatography column at room temperature, indicate that gold efficiently traps even the most volatile polonium species formed in moist helium atmosphere at low temperatures. However, it cannot be completely ruled out that adsorption mechanisms are different at high and low temperature. Therefore, we recommend that the trapping efficiency of polonium on gold surfaces at low temperature should be studied in more detail, e.g. by isothermal gas chromatography.

**Acknowledgments:** This work was supported by the project SEARCH, co-funded by the European Commission under the Seventh Euratom Framework Programme for Nuclear Research & Training Activities (2007–2011) under Contract Number 295736.

## References

1. Cohen, B. L.: Risk analysis of buried waste from electricity generation. *Am. J. Phys.* **54**, 38 (1986).
2. González-Romero, E. M.: Impact of partitioning and transmutation on the high level waste management. *Nucl. Eng. Des.* **241**, 3436 (2011).
3. Salvatores, M., Palmiotti, G.: Radioactive waste partitioning and transmutation within advanced fuel cycles: achievements and challenges. *Prog. Part. Nucl. Phys.* **66**, 144 (2011).
4. Rubbia, C.: A high gain energy amplifier operated with fast neutrons. *AIP Conf. Proc.* **346**, 44 (1995).
5. Sasa, T.: Research activities for accelerator-driven transmutation system at JAERI. *Prog. Nucl. Energ.* **47**, 314 (2005).
6. Magill, J., Pfennig, G., Dreher, R., Söti, Z.: Karlsruhe Nuklidkarte/Chart of the Nuclides. 9th ed. Nucleonica GmbH, Eggenstein-Leopoldshafen (2015).
7. Colle, R., Fitzgerald, R. P., Laureano-Perez, L.: A new determination of the Po-209 half-life. *J. Phys. G Nucl. Part. Phys.* **41**, 105103 (2014).
8. Naimark, D. H.: Effective half-life of polonium in the human, Technical Report MLM-272/XAB, Mound Lab., Miamisburg, OH. MLM-272/XAB; Other: CNN: AEC-AT-33-1-GEN-53 United States Other: CNN: AEC-AT-33-1-GEN-53 Tue Feb 12 16:32:19 EST 2008NTISGRA; GRA-94-31659; EDB-94-119176 English, 1949.

9. Neuhausen, J., Köster, U., Eichler, B.: Investigation of evaporation characteristics of polonium and its lighter homologues selenium and tellurium from liquid Pb-Bi-eutectic. *Radiochim. Acta* **92**, 917 (2004).
10. Gonzalez Prieto, B., Van den Bosch, J., Martens, J. A., Neuhausen, J., Aerts, A.: Equilibrium evaporation of trace polonium from liquid lead-bismuth eutectic at high temperature. *J. Nucl. Mater.* **450**, 299 (2014).
11. Buongiorno, J., Larson, C., Czerwinski, K. R.: Speciation of polonium released from molten lead bismuth. *Radiochim. Acta* **91**, 153 (2003).
12. Ohno, S., Kurata, Y., Miyahara, S., Katsura, R., Yoshida, S.: Equilibrium evaporation behavior of polonium and its homologue tellurium in liquid lead-bismuth eutectic. *J. Nucl. Sci. Technol.* **43**, 1359 (2006).
13. Petryanov, I. V., Borisov, N. B., Churkin, S. L., Borisova, L. I., Starostina, I. A.: Generation and isolation of gaseous fraction of polonium from its solid preparations. *Dokl. Akad. Nauk SSSR* **322**, 557 (1992).
14. Maugeri, E. A., Neuhausen, J., Eichler, R., Piguët, D., Mendonça, T. M., Stora, T., Schumann, D.: Thermochemistry study of volatile polonium species in various gas atmospheres. *J. Nucl. Mater.* **450**, 292 (2014).
15. Pankratov, D. V., Efimov, E. I., Toshinskii, G. I., Ryabaya, L. D.: Analysis of the polonium hazard in nuclear power systems with lead–bismuth coolant. *At. Energ.* **97**, 559 (2004).
16. Buongiorno, J., Loewen, E. P., Czerwinski, K., Larson, C.: Studies of polonium removal from molten lead-bismuth for lead-alloy-cooled reactor applications. *Nucl. Technol.* **147**, 406 (2004).
17. Heinitz, S., Neuhausen, J., Schumann, D.: Alkaline extraction of polonium from liquid lead bismuth eutectic. *J. Nucl. Mater.* **414**, 221 (2011).
18. Heinitz, S.: Investigations on physico-chemical aspects of lead-based alloys for nuclear applications. (Ph.D. Thesis), University of Bern (2013).
19. Obara, T., Koga, T., Miura, T., Sekimoto, H.: Polonium evaporation and adhesion experiments for the development of polonium filter in lead–bismuth cooled reactors. *Prog. Nucl. Energ.* **50**, 556 (2008).
20. Gäggeler, H., Dornhofer, H., Schmidt-Ott, W. D., Greulich, N., Eichler, B.: Determination of adsorption enthalpy for polonium on surfaces of copper, silver, gold, palladium and platinum. *Radiochim. Acta* **38**, 103 (1985).
21. Rona, E.: Verdampfungsversuche an polonium. *Sitzungsber. Akad. Wiss., Wien* **141**, 533 (1932).
22. Rona, E., Hoffer, M.: Verdampfungsversuche an Polonium in Sauerstoff und Stickstoff. *Sitzungsber. Akad. Wiss. Wien* **144**, 397 (1935).
23. Eichler, B., Gäggeler, H., Rossbach, H., Hübener, S.: Adsorption of volatile metals on metal surfaces and its application in nuclear chemistry. 2. Evaluation of adsorption enthalpies for polonium on surfaces of transition metals and copper, silver and gold. *Radiochim. Acta* **38**, 131 (1985).
24. Zvara, I.: The inorganic radiochemistry of heavy elements. Springer, Netherlands (2010).
25. Eichler, B., Zude, F., Fan, W., Trautmann, N., Herrmann, G.: Complex transport reactions in a temperature gradient tube: radiochemical study of volatilization and deposition of Iridium oxides and hydroxides. *Radiochim. Acta* **61**, 81 (1993).
26. Zvara, I.: Simulation of thermochromatographic processes by the Monte Carlo method. *Radiochim. Acta* **38**, 95 (1985).
27. Eichler, B.: The behaviour of radionuclides in gas adsorption chromatographic processes with superimposed chemical reactions (chlorides). *Radiochim. Acta* **72**, 19 (1996).
28. Greenwood, N. N., Earnshaw, A.: Chemistry of the elements. Pergamon press, Oxford (1984).
29. Rijpstra, K.: Density functional theory as a tool to get more out of experimental data: case-studies for Al-Zn-O and for the interaction between Po and Po-Bi-eutectic. (Ph.D. Thesis), Faculteit Wetenschappen Vakgroep Natuurkunde & Sterrenkunde, Universiteit Gent (2014).
30. Eichler, B.: Bestimmung der Adsorptionswärmen gasförmiger Metalle auf festen Metalloberflächen bei Null-Bedeckung. Zentralinstitut für Kernforschung, Rossendorf (1978).
31. Neuhausen, J., Eichler, R.: Extension of Miedema's macroscopic atom model to the elements of group 16 (O, S, Se, Te, Po) PSI Report No. 03–13. PSI, Villigen (2003).
32. de Boer, F. R., Boom, R., Mattens, W. C. M., Miedema, A. R., Niessen, A. K.: Cohesion in metals, transition metal alloys. North-Holland, Amsterdam (1988).
33. Eichler, B., Rossbach, H.: Adsorption of volatile metals on metal surfaces and its application in nuclear chemistry. 1. Calculation of adsorption enthalpies for hypothetical superheavy elements with Z around 114. *Radiochim. Acta* **33**, 121 (1983).
34. Abakumov, A. S.: Thermal reactions of polonium. *Russ. Chem. Rev.* **51**, 622 (1982).
35. Fazio, C.: Handbook on lead-bismuth eutectic alloy and lead properties, materials compatibility, thermal-hydraulics and technologies – 2015 Edition, OECD/NEA Nuclear Science Committee (2015).
36. González Prieto, B.: Evaporation of polonium from lead-bismuth eutectic nuclear coolant, PhD, Bioscience Engineering, KU Leuven (2015).
37. Rizzi, M., Neuhausen, J., Eichler, R., Tuerler, A., Mendonça, T. M., Stora, T., Prieto, B. G., Aerts, A., Schumann, D.: Polonium evaporation from dilute liquid metal solutions. *J. Nucl. Mater.* **450**, 304 (2014).

**Supplemental Material:** The online version of this article (DOI: 10.1515/ract-2016-2573) offers supplementary material, available to authorized users.